NASA-TM-107074
19960011375

NASA Technical Memorandum 107074

Planar Imaging of Hydroxyl in a High Temperature, High Pressure Combustion Facility

Yolanda R. Hicks
Lewis Research Center
Cleveland, Ohio

Randy J. Locke
NYMA, Inc.
Brook Park, Ohio

Robert C. Anderson
Lewis Research Center
Cleveland, Ohio

Kelly A. Ockunzzi
Ohio Aerospace Institute
Cleveland, Ohio

Prepared for the
International Symposium on Optical Science, Engineering and Instrumentation
sponsored by the Society of Photo-Optical Instrumentation Engineers
San Diego, California, July 9–14, 1995

National Aeronautics and
Space Administration

Planar Imaging of Hydroxyl in a High Temperature, High Pressure Combustion Facility

Yolanda R. Hicks
NASA Lewis Research Center
Cleveland, Ohio 44135

Randy J. Locke
NYMA, Inc.
Engineering Services Division
Brook Park, Ohio 44142

Robert C. Anderson
NASA Lewis Research Center
Cleveland, Ohio 44135

Kelly A. Ockunzzi
Ohio Aerospace Institute
Cleveland, Ohio 44142

ABSTRACT

An optically accessible flame tube combustor is described which has high temperature, pressure, and air flow capabilities. The windows in the combustor measure 3.8 cm axially by 5.1 cm radially, providing 67% optical access to the square cross section flow chamber. The instrumentation allows one to examine combusting flows and combustor subcomponents, such as fuel injectors and air swirlers. These internal combustor subcomponents have previously been studied only with physical probes, such as temperature and species rakes. Planar laser-induced fluorescence (PLIF) images of OH have been obtained from this lean burning combustor burning JP-5 fuel. These images were obtained using various laser excitation lines of the OH A←X (1,0) band for two fuel injector configurations with pressures ranging from 1013 kPa (10 atm) to 1419 kPa (14 atm), and equivalence ratios from 0.41 to 0.59. Non-uniformities in the combusting flow, attributed to differences in fuel injector configuration, are revealed by these images.

1. INTRODUCTION

The powerplants for the next generation supersonic aircraft are mandated to meet strict performance requirements. Efforts at NASA Lewis Research Center include reducing combustion emissions, specifically NO_x and CO, while improving combustor efficiency. NO_x reduction is targeted because NO_x is believed to destroy stratospheric ozone[1]. The next generation combustors will operate at higher temperatures and pressures than current combustors. While these operating conditions should lead to greater engine efficiency, they pose technical challenges in the reduction of NO_x[2,3]. To lower emissions, an improved understanding of the combustion process at these operating conditions is necessary, but these extreme conditions pose unique challenges to all established combustor diagnostic methods.

Established methods of analyzing engine performance use gas sampling to measure combustion efficiency and smoke. Standard gas analysis equipment measures CO, CO_2, H_2O, O_2, NO, NO_2, and unburned hydrocarbons. However, these instruments cannot directly probe the combustor to reveal flame structure or to see the underlying processes that lead to good or bad efficiency. Significant kinetics information is lost as well, because physical probes can measure only stable species. Combustion modelers are interested in hydroxyl (OH) as a major combustion intermediate, and because of its importance in the thermal NO formation mechanism[3,4]. Combustor designers are interested in OH as well, particularly as a flame zone marker. OH provides a relative scale of temperature, because its presence indicates where combustion occurs, and therefore where heat is released. In addition to its importance in the thermal NO_x formation mechanism, temperature plays a key role in engine lifetime. The spatial distribution of temperature is important because radiative and convective heat transfer affect survivability and lifetime of key combustor subcomponents, such as the dome and liner. Hot spots can play a deleterious role at the combustor exit by harming the turbine

material. A non-uniform temperature distribution is also evidence of poor mixing of the fuel and air within the combustor. Good mixing is a key factor in achieving high combustor performance and efficiency[5,6].

Laser-based diagnostic techniques have demonstrated the capability to supply nonintrusive information on such diverse parameters as species concentration, temperature, velocity, and pressure[7]. Of these methods, planar laser-induced fluorescence (PLIF) offers the potential to acquire temporally resolved, two-dimensional species, temperature and velocity measurements, all of which are of considerable value to research in advanced gas turbine combustor design. A large research base has been established in PLIF diagnostics of gaseous flows at atmospheric pressure. This work includes PLIF imaging of the flame front and various molecular species in premixed and diffusion flames[8,9]. Species imaging with PLIF has also been extended to high pressure gaseous flames[10]. Recent experiments have captured PLIF images from atmospheric[11] and high pressure spray flames[12].

This paper describes a unique, optically-accessible combustor operating on JP-5 fuel at realistic flight operating conditions for future supersonic aircraft, and presents preliminary qualitative PLIF images of hydroxyl which reveal the flame structure resulting from different fuel injector configurations.

2. EXPERIMENTAL APPARATUS

2.1 Flame Tube Combustor Facility

The combustor facility supplies non-vitiated air at flow rates of up to 10 pounds per second. Four natural gas can-type burners provide combustor air inlet temperatures between 589 K and 866 K to the windowed lean flame tube combustor. A schematic of the combustor is shown in figure 1. The subcomponents that can be varied in this rig are the fuel injectors, either in number or in style of injection. The combustor measures 74 cm in length and has a 7.62 cm x 7.62 cm (3 in. x 3 in.) cross section flowpath, with a flow area of 58.06 cm^2. Its housing is water-cooled. The liner is made using an aluminum oxide castable ceramic material, typically Greencast 94+. Four window assemblies, circumferentially 90 degrees apart, are located such that the centers of the windows are 14.3 cm downstream of the combustor inlet. The combustor is outfitted with up to four 1.27 cm thick ultraviolet grade fused silica windows, each with a clear aperture of 3.8 cm x 5.1 cm. This grade of quartz has a minimum light transmissivity of 80% over the spectral range from 180 nm to 3300 nm.

The window assemblies are designed to withstand flame temperatures up to 2033 K (3200 °F) and rig pressures up to 2068.1 kPa (300 psia). The maximum ignition thermal cycle allows for a ΔT of 889 K (1600°F), from an inlet temperature of 867 K (1100 °F) to an ignition temperature of 1756 K (2700 °F). Water cooling and nitrogen film cooling are used to ensure that the windows can survive this severe environment. The nitrogen film cooling mechanism provides no more than 10% of the aggregate combustor mass flowrate.

2.2 Laser Diagnostics Facility

2.2.1 Laser Systems

The laser diagnostics facility consists of pulsed and continuous wave lasers, triggering and timing electronics, optics, photodetectors, cameras and other detection equipment, traversing stages, and system calibration devices. Laser systems include: (1) A Nd:YAG pumped dye laser system with frequency doubling, mixing, or mixing after doubling. Its tunable wavelength range is 220 nm to 560 nm, and it has a pulse repetition rate of 10 Hz; (2) A XeCl Excimer pumped dye laser system, with a tunable wavelength range, after doubling, of 220 nm to 300 nm. Its pulse repetition rate is 100 Hz; (3) A 5 watt continuous wave Argon-Ion Laser.

2.2.2 Laser Beam Transport System

Due to safety concerns, the laser systems must be operated remotely from the test cell. This necessitates a complex scheme, utilizing a series of mirrors and traversing stages, to direct the beam into the flame tube at the desired location. Figure 2 illustrates the laser diagnostics facility beam transport system and the path the laser beam(s) must take. The beam travels upward from the table in the laser room, above and across the control room into the test cell, and down into the appropriate location in the test rig. With the aid of figure 2, the following text describes how that is achieved.

Upon leaving the table the laser beam is positioned using mirrors with DC motorized actuators and a three-axis positioning system, all mounted from the ceiling. The mirror mounts have horizontal and vertical tilt control, with a resolution of < 0.05 μm. The first mirror is positioned directly above the laser room, and transmits the beam from the table into the test cell through a shuttered

hole in the wall. Upon entering the test cell, the beam projects over the inlet region, approximately 110 cm upstream of the window location. Therefore, a second mirror receives the beam and directs it downstream, parallel to the test rig axis, to the final mirror, which is positioned directly over the top window in the flame tube. The final mirror steers the beam through sheet forming optics and into the flame tube.

A table installed on the ceiling of the test cell is used to position the second and third mirrors. The table consists of three motorized stages. Two of the stages control the axial positioning of the beam. They in turn are mounted on the third stage, which controls the lateral positioning of the beam. The first of the axial stages controls the axial position of the second mirror. The second stage moves the third mirror.

The beam path, from the laser table optics until the beam enters the test cell area, is enclosed. This enclosure can be purged with nitrogen in order to minimize absorption (loss) of laser energy at wavelengths that are strongly absorbed by diatomic oxygen.

2.2.3 Detection System

The laser sheet is imaged from 90° with an intensified CCD camera focused through a side window. As with the input beam, the position of the camera is remotely controlled. The camera is typically mounted on a three-axis system of translating stages situated next to the combustor.

2.2.4 Position Control

To reduce the complexity of positioning the laser beam and detector, all stages are controlled with a computer through a program written to coordinate their movement. The program was written using LabWindows/CVI, a software development tool produced by National Instruments. The program allows the user to select which laser beam and detector configuration are used in the test run. The user can specify the type and orientation of each stage mounted in the test cell and how the stages are connected to the motion controllers. Based on these selections, the program correctly controls the distance and direction the stages move. The user can position the laser beam in terms of rectangular coordinates using fractions of millimeters. Movement of the detector is coordinated so the image remains in focus. The program records the coordinates the user enters, as well as any test conditions the user wants to document, in a file specified by the user. The user can also define an origin, so the coordinates entered correspond to the position of the laser beam in the test region. The origin is also recorded, so that it can be reproduced for the next test run or in case a power failure occurs and the current position of the stages is not known.

3. EXPERIMENTAL PROCEDURE

The lasers used for acquiring the OH PLIF images consisted of a Continuum Nd:YAG-pumped (NY-81C) dye laser (ND60), whose output was doubled to provide the desired UV radiation. The YAG laser 2nd harmonics provided approximately 750 mJ per pulse at 10 Hz. The dye laser, using R590 dye, produced pulses of 180 mJ at 564 nm. The dye laser output was frequency doubled to 283 nm by a nonlinear BBO crystal in a Continuum UVX frequency doubler/mixer in a UVT-1 configuration. Its output was approximately 16 mJ per pulse with a bandwidth of 1.0 cm^{-1}, as measured by a Burleigh UV pulsed wavemeter. The UV light was separated from the residual dye output by a pellin-broca prism. The dye laser was tuned to one of three specific rovibronic transitions of the OH A←X(1,0) band, $R_1(1)$@281.458 nm, $R_1(10)$@281.591 nm, and $Q_1(1)$@281.970 nm. The desired transition was verified by directing the laser beam through the flame of a Bunsen burner at atmospheric pressure and observing the fluorescence with a photomultiplier tube/boxcar averager system. The doubled dye output was expanded and collimated to approximately 2 cm in diameter and directed through the beam transport system.

Sheet forming optics consisted of a spherical lens combination for beam sizing coupled with a cylindrical lens with a 3 m focal length. The resultant focused laser sheet had dimensions of 33 mm x 0.3 mm. Laser energy, prior to entering the test section, was approximately 10 mJ distributed over the sheet and approximated a Gaussian distribution. Laser energy at the laser focal volume within the test section depended upon the cleanliness of the windows and upon refractive effects of the turbulent combustion process.

The fluorescence from OH was collected at 90° from the laser sheet by a 105 mm, f/4.5 UV Nikkor lens attached to a Princeton Instruments intensified CCD camera with an array size of 576 x 384 pixels. The field of view of the camera was large enough to view the entire collection window. The camera intensifier was synchronously triggered with the laser pulse and was gated for 50 ns. A combination of a WG-305 Schott glass filter (2 mm) and a narrow band interference filter from Andover Corp. #313FS10-50 (2 mm), with a peak wavelength of 315 nm and a FWHM of 10.6 nm, was used to collect OH fluorescence while efficiently eliminating scattered laser light. Princeton Instrument's WinView software was used to acquire the ICCD images.

The fuel injection system consisted of Lean Direct Injection (LDI), with nine discrete fuel injection points. In LDI concepts, the fuel is emitted directly into the reaction zone. Swirl is imparted to the air, and in some cases also to the fuel, to generate a recirculation zone that is used to stabilize the flame. Two different air swirl schemes were examined. One configuration used 45° swirl. The other had a combination of 60° and 45° swirl, abbreviated to 60°/45°.

The combustor was tested under the following range of parameters. The inlet temperature was varied from 811 K to 866 K, with combustor pressures from 1034 kPa to 1413 kPa. These were supported by air flow rates of 0.59 to 0.83 kg/s. JP-5 fuel was matched to the appropriate air flow rates at a given temperature and pressure to achieve equivalence ratios,Φ, of 0.41, 0.47, 0.50, and 0.53.

4. IMAGE ANALYSIS

The images were processed on a Silicon Graphics Indigo workstation using PV-WAVE data visualization software from Visual Numerics, Inc. Subroutines have been developed to read the WinView image format and convert each image into an array usable by PV-WAVE. For displays using a 256-color palette, the images are scaled so that the minimum is 0 and the maximum is 255. For the results presented herein, image processing includes background subtraction and removal of noise spikes.

Background subtraction effectively reduces the minimum pixel value for an image to near zero by subtracting from each image pixel value a background image's corresponding pixel value. When a background image is not available the image minimum value is subtracted from all pixels. Removal of image noise spikes is necessary in these experiments due to their adverse affect upon any scaling routine. The cause of the spikes is currently unknown, but particulate emission and electrical noise on long cables from camera to acquisition electronics are possible causes. The noise spikes appear as an island of 1 or 2 pixels with a value much higher than that of surrounding pixels. The spike noise removal routine works by changing the value of all pixels which satisfy the removal condition to the image minimum value. The removal condition depends on the image histogram. For an image represented by an integer array, each pixel value on the scale from image minimum to image maximum has its own histogram bin. A pixel is marked for removal if its value puts it into a histogram bin above that group of bins containing 99% of all pixel values.

5. RESULTS AND DISCUSSION

With the exception of figures 6 and 7, each image within a figure has been normalized to that image within the figure with the highest pixel value. In all cases, the laser sheet passes vertically, from top to bottom. The flow passes from left to right. The images obtained in this study are qualitative in nature. Therefore, the OH images portray relative fluorescent yields only.

The PLIF images were obtained with the camera positioned so that the collection window was centered in its field of view, with the illuminated flowfield at its focus. The upstream edge of the windows corresponds to a position approximately 13 cm downstream of the fuel injector exit plane. Equilibrium code calculations[13] for the range of test conditions used in this study have predicted OH concentrations on the order of 300 ppm in the flame zone.

Figure 3 shows a comparison among the three resonant excitation lines used, $R_1(1)$, $R_1(10)$, and $Q_1(1)$, respectively. The three lines were chosen as candidate excitations for two reasons. First, they are all strong lines in the atmospheric flame and provide a good basis for looking at the higher pressure flame confined within the combustor. Second, they lie within 0.5 nm of one another. The small separation is important because as the laser is scanned to select an appropriate wavelength, a small angular deviation in output direction results. When the distance to the experiment is short, the angular variation may be unimportant. The beam in this experiment must travel approximately 24 meters to reach the test rig, and such a long lever arm magnifies what appear to be minute or even nonevident shifts in beam position. Each image in figure 3 was obtained with an inlet temperature of 866 K, combustor pressure of 1034 kPa, 60°/45° air swirl, and Φ of 0.53. The plots immediately below each image give that image's relative pixel intensity from top to bottom (which corresponds to the direction of laser beam travel) along the white lines in each image. Neither the $R_1(1)$ nor the $R_1(10)$ line shows indication of laser sheet attenuation. The $Q_1(1)$ line, however, displays strong evidence of laser beam attenuation, on the order of 40%. Facility operating procedures preclude the possibility of calibrating the camera CCD with a known intensity gradient in situ prior to a test run. Therefore, to determine an accurate OH distribution, a transition that displays minimal laser absorption should be selected. Although the $R_1(1)$ and $R_1(10)$ excitation lines display little attenuation, the $R_1(1)$ line has a low fluorescence yield compared to the $R_1(10)$ line. Based upon the representative candidate images of figure 3, $R_1(10)$ was selected for subsequent imaging of OH.

Figure 4 shows a comparison between resonant and off-resonant excitation with 60°/45° swirl. The resonant excitation line is $R_1(10)$ at 281.591. The off-resonant excitation is at 281.01 nm. Each image is composed of ten laser pulses. The combustor

pressure was 1034 kPa and Φ was 0.53. The off-resonant image shows no evidence of either elastically scattered laser light or contributions attributable to complex fuel chemistries and/or polycyclic aromatic hydrocarbons. Therefore, the resonant PLIF signal is attributable only to fluorescence from OH.

Figure 5 is a comparison of OH PLIF images acquired at the same flow conditions but at different equivalence ratios. The combustor used the 60°/45° air swirl configuration. The inlet temperature was 866 K, the mass flow rate of air was 0.83 kg/s, and the combustor pressure was 1398 kPa. The equivalence ratios are 0.53, 0.50, 0.47, and 0.41, respectively. The images consist of an average of 10 laser pulses. Each image was normalized for WinView autoscaling routine differences, thus presenting an accurate representation of the relative fluorescence intensity. As expected, the OH fluorescence intensity dramatically diminishes with decreasing equivalence ratio. One can also see that the amount of hydroxyl formed is relatively uniform across the flowfield for this injector configuration. That is not the case with a different swirler configuration. Figure 6 shows a comparison of 60°/45° and 45° swirl. More OH is formed toward the walls of the combustor for the 45° swirl, with relatively low amounts formed at the centerline. This corresponds with higher temperatures along the walls of the combustor, rather than in the center, and indicates potential problems in keeping the liner cool. Further examination of that configuration using a series of single laser pulses, shown in figure 7, reveals that "lobes" of high OH are formed asymmetrically. Sometimes, a single lobe appears at the top of the combustor, sometimes at the bottom, and other instances, it occurs at both the top and bottom of the flame tube. These data show that the nature of the combustion is not necessarily uniform and that, on the microscale, the flow is random. This finding was subsequently substantiated by Computational Fluid Dynamics calculations. Gas sampling of the combustor emissions had earlier revealed that the 60°/45° air swirl configuration performed better than did the 45° swirl configuration. However, it could provide no explanation of why. These images vividly illustrate that the 45° air swirl configuration does a comparatively poor job of mixing fuel and air. This information can only be obtained by optical means, and it enhances the ability to understand combustion processes in a realistic system, and therefore predict combustion phenomena and design combustors more easily.

6. CONCLUSIONS

These results demonstrate the viability of the planar laser-induced fluorescence diagnostic technique applied to an actual high pressure, high temperature combustion facility. This is the only facility of its kind, capable of providing advanced diagnostics for design and optimization of gas turbine combustors. PLIF images of OH were obtained at a range of test conditions duplicating those to be experienced in future high performance combustors. The PLIF results of OH using different lean direct injection configurations has shown that the fluid mechanics within the combustor are highly turbulent, and that there are large fluctuations in hydroxyl, and consequently temperature, on the microscale. This information is important for combustor design and kinetics modeling, and provides details that are impossible to determine with traditional physical probes.

7. FUTURE WORK

Future experiments will explore additional excitation lines and fluorescence signal detection filtering options. PLIF will be extended to measure temperature and other species of interest, such as CH and NO. The maximum combustor operating pressure will be extended to 2026 kPa (20 atm).

8. REFERENCES

1. H.S. Johnston, E.D. Kinnison, and D.J.Wuebbles, "Nitrogen oxides from high-altitude aircraft: an update of potential effects on ozone," *Journal of Geophysical Research*, **94**, Number D13, pp. 16351–16363, 20 Nov. 1989.
2. R.R. Tacina, "Low NO_x potential of gas turbine engines," AIAA Paper No. 90–0550, 28th Aerospace Sciences Meeting and Exhibit, Reno, Nevada, January 1990.
3. S.M. Correa, "A review of NO_x formation under gas-turbine combustion conditions," *Combust. Sci. and Tech.*, **87**, pp. 329–362, 1992.
4. J.A. Miller and C.T. Bowman, "Mechanism and modeling of nitrogen chemistry in combustion," *Prog. Eng. Combust. Sci.*, **15**, pp. 287–338, 1989.
5. C.-M. Lee, W.J. Ratvatsky, R.J. Locke, and B. Ghorashi, "Effect of fuel-air mixing upon NO_x emissions for a lean premixed prevaporized combustion system," NASA TM 105980, 1993.

6. A.H. Lefebvre, *Gas Turbine Combustion*, pp.123–177, Hemisphere Publishing Corporation, New York, 1983.
7. R.K. Hanson, "Combustion diagnostics: planar imaging techniques," *Twenty-First Symp.(Int'l) on Combustion*, pp. 1677–1691, The Combustion Institute, 1986.
8. P.H. Paul, U.E. Meier, and R.K. Hanson, "Single-shot, multiple-camera planar laser-induced fluorescence imaging in gaseous flows," AIAA Paper No. 91–0459, 29th Aerospace Sciences Meeting and Exhibit, Reno, Nevada, January 1991.
9. J.M. Seitzman, J.L. Palmer, A.L. Antonio, R.K. Hanson, P.A. DeBarber, and C.F. Hess, "Instantaneous planar thermometry of shock-heated flows using PLIF of OH," AIAA Paper No. 93–0802, 31st Aerospace Sciences Meeting and Exhibit, Reno, Nevada, January 1993.
10. B.E. Battles, J.M. Seitzman, and R.K. Hanson, "Quantitative planar laser-induced fluorescence imaging of radical species in high pressure flames," AIAA Paper No. 94–0229, 32nd Aerospace Sciences Meeting and Exhibit, Reno, Nevada, January 1994.
11. A. Koch, A. Chryssostomou, P. Andresen, and W. Bornscheuer, "Multi-species detection in spray flames with tunable excimer lasers," *Applied Physics B*, **56**, No. 3, p. 165, 1993.
12. M.G. Allen, K.R. McManus, and D.M. Sonnenfroh, "PLIF imaging in spray flame combustors at elevated pressure", AIAA Paper No. 95–0172, 33rd Aerospace Sciences Meeting and Exhibit, Reno, Nevada, January 1995.
13. S. Gordon and B.J. McBride, "Computer program for calculation of complex chemical equilibrium compositions, rocket performance, incident and reflected shocks, and chapman-jouget detonations," *NASA SP–273*, 1971.

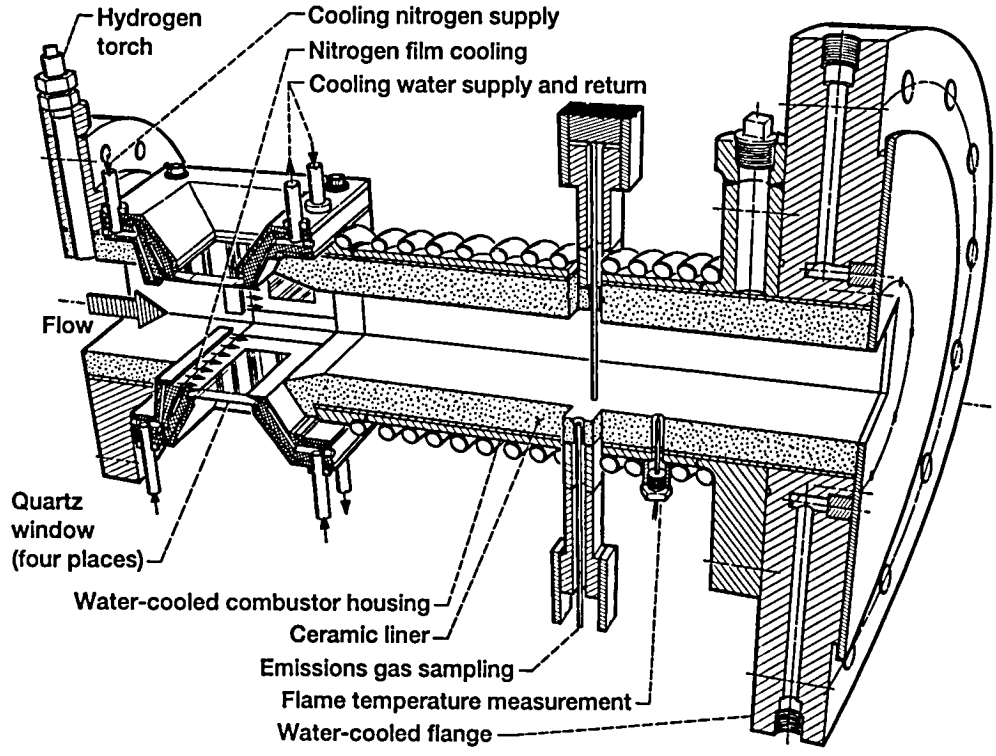

Figure 1.—Thin film cooled, optically accessible flame tube combustor.

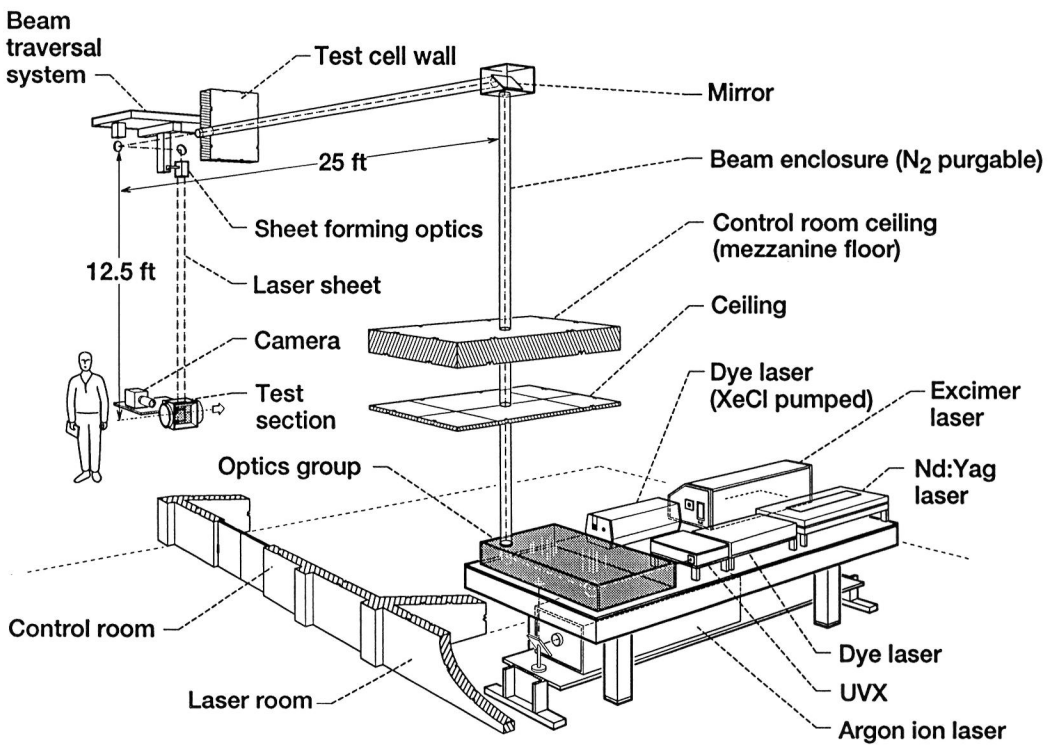

Figure 2.—Beam transport system.

Page intentionally left blank

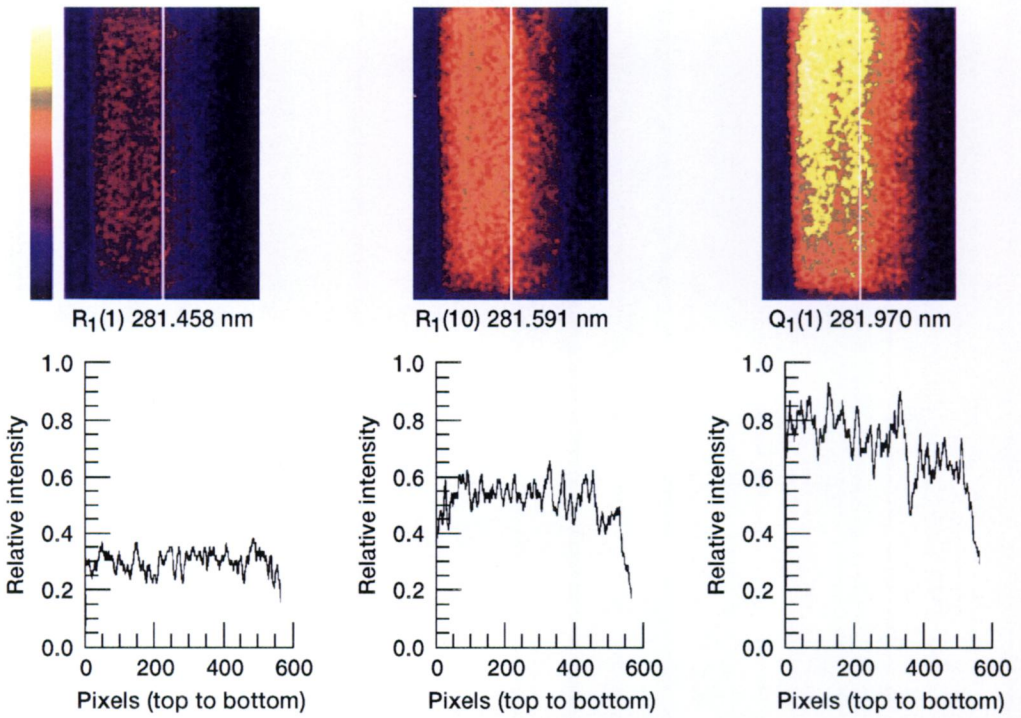

Figure 3.—Comparison of OH PLIF images with different resonant excitation for 9 pt LDI with 60°/45° swirl at P_{in} = 1034 kPa, T_{in} = 866 °K, and ϕ = 0.53.

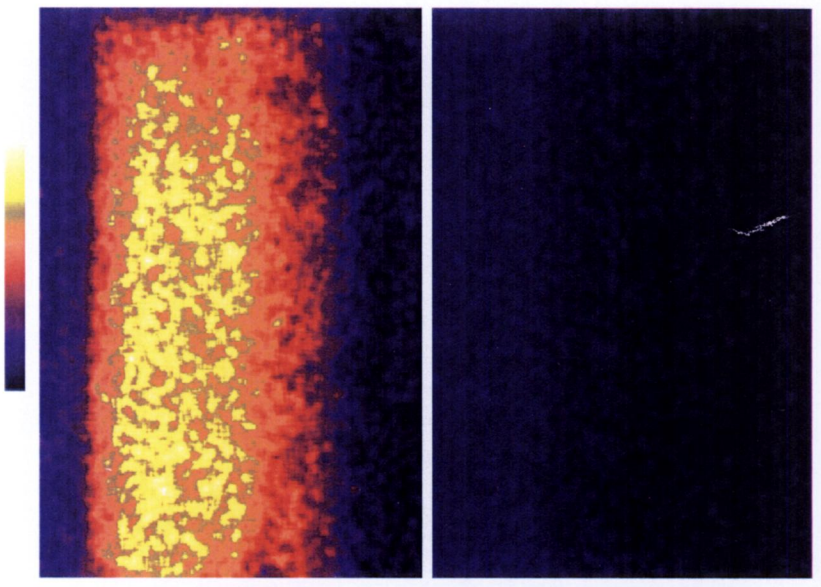

Figure 4.—Comparison of resonant and non-resonant OH PLIF images for 9 pt LDI with 60°/45° swirl at P_{in} = 1034 kPa, T_{in} = 866 °K, and ϕ = 0.53. Resonant excitation is $R_1(10)$.

Page intentionally left blank

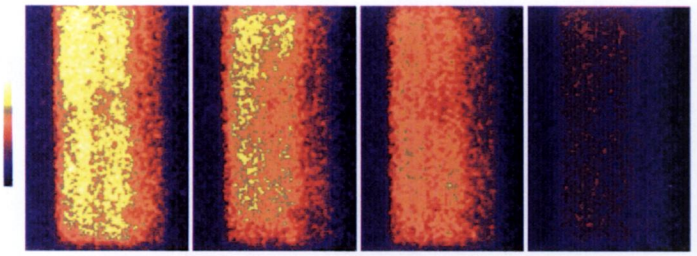

Figure 5.—Comparison of OH PLIF images for different equivalence ratios with 9 pt LDI and 60°/45° swirl at P_{in} = 1379 kPa, T_{in} = 866 °K. Resonant excitation is $R_1(10)$.

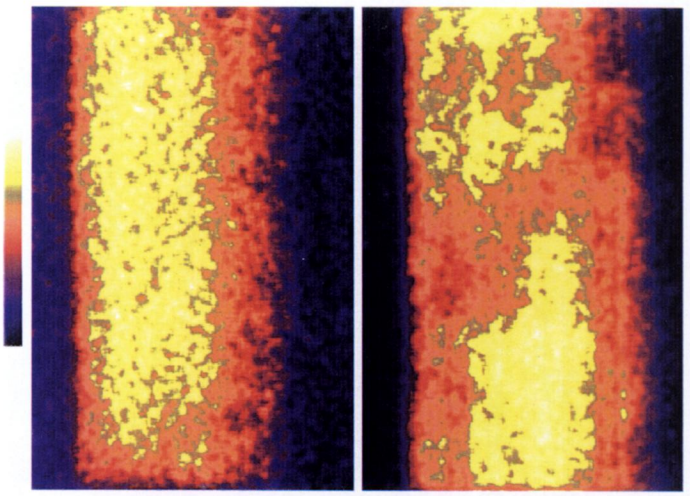

Figure 6.—Comparison of OH PLIF images for different fuel injector configurations with 9 pt LDI at P_{in} = 1034 kPa, T_{in} = 866 °K, and ϕ = 0.53. Resonant excitation is $R_1(10)$.

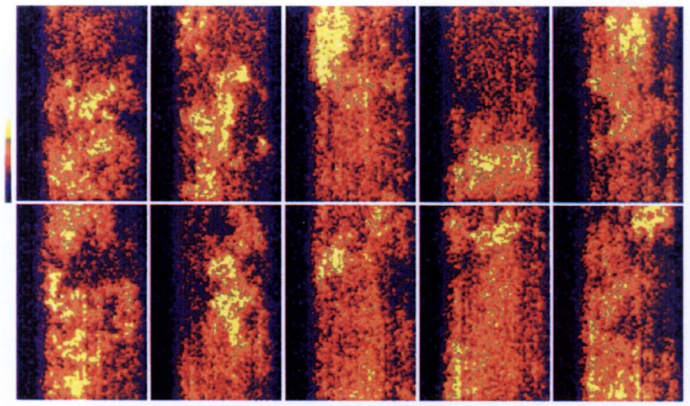

Figure 7.—Shot-to-shot variation in flame structure for 9 pt LDI with 45° swirl, P_{in} = 1034 kPa, T_{in} = 866 °K, and ϕ = 0.41. Resonant excitation is $R_1(10)$.

REPORT DOCUMENTATION PAGE

Form Approved
OMB No. 0704-0188

1. AGENCY USE ONLY (*Leave blank*)	2. REPORT DATE	3. REPORT TYPE AND DATES COVERED
	October 1995	Technical Memorandum

4. TITLE AND SUBTITLE
Planar Imaging of Hydroxyl in a High Temperature, High Pressure Combustion Facility

5. FUNDING NUMBERS
WU-537-02-20

6. AUTHOR(S)
Yolanda R. Hicks, Randy J. Locke, Robert C. Anderson, and Kelly A. Ockunzzi

7. PERFORMING ORGANIZATION NAME(S) AND ADDRESS(ES)
National Aeronautics and Space Administration
Lewis Research Center
Cleveland, Ohio 44135-3191

8. PERFORMING ORGANIZATION REPORT NUMBER
E-9938

9. SPONSORING/MONITORING AGENCY NAME(S) AND ADDRESS(ES)
National Aeronautics and Space Administration
Washington, D.C. 20546-0001

10. SPONSORING/MONITORING AGENCY REPORT NUMBER
NASA TM-107074

11. SUPPLEMENTARY NOTES
Prepared for the International Symposium on Optical Science, Engineering and Instrumentation sponsored by the Society of Photo-Optical Instrumentation Engineers, San Diego, California July 9-14, 1995. Yolanda R. Hicks, and Robert C. Anderson, NASA Lewis Research Center; Randy J. Locke, NYMA, Inc., 2001 Aerospace Parkway, Brook Park, Ohio 44142 (work funded by NASA Contract NAS3-25266); Kelly A. Ockunzzi, Ohio Aerospace Institute, 22800 Cedar Point Road, Cleveland, Ohio 44142. Responsible person, Yolanda R. Hicks, organization code 2710, (216) 433-3410.

12a. DISTRIBUTION/AVAILABILITY STATEMENT
Unclassified - Unlimited
Subject Categories 07, 34, and 35

This publication is available from the NASA Center for Aerospace Information, (301) 621-0390.

12b. DISTRIBUTION CODE

13. ABSTRACT (*Maximum 200 words*)

An optically accessible flame tube combustor is described which has high temperature, pressure, and air flow capabilities. The windows in the combustor measure 3.8 cm axially by 5.1 cm radially, providing 67% optical access to the square cross section flow chamber. The instrumentation allows one to examine combusting flows and combustor subcomponents, such as fuel injectors and air swirlers. These internal combustor subcomponents have previously been studied only with physical probes, such as temperature and species rakes. Planar laser-induced fluorescence (PLIF) images of OH have been obtained from this lean burning combustor burning Jet-A fuel. These images were obtained using various laser excitation lines of the OH A←X (1,0) band for two fuel injector configurations with pressures ranging from 1013 kPa (10 atm) to 1419 kPa (14 atm), and equivalence ratios from 0.41 to 0.59. Non-uniformities in the combusting flow, attributed to differences in fuel injector configuration, are revealed by these images.

14. SUBJECT TERMS	15. NUMBER OF PAGES
Optically accessible modular combustor; Planar laser-induced fluorescence of OH	11
	16. PRICE CODE: A03

17. SECURITY CLASSIFICATION OF REPORT	18. SECURITY CLASSIFICATION OF THIS PAGE	19. SECURITY CLASSIFICATION OF ABSTRACT	20. LIMITATION OF ABSTRACT
Unclassified	Unclassified	Unclassified	